325
2/20/64

IDO-14621

MASTER

CHEMICAL PROCESSING TECHNOLOGY QUARTERLY PROGRESS REPORT

April - June, 1963

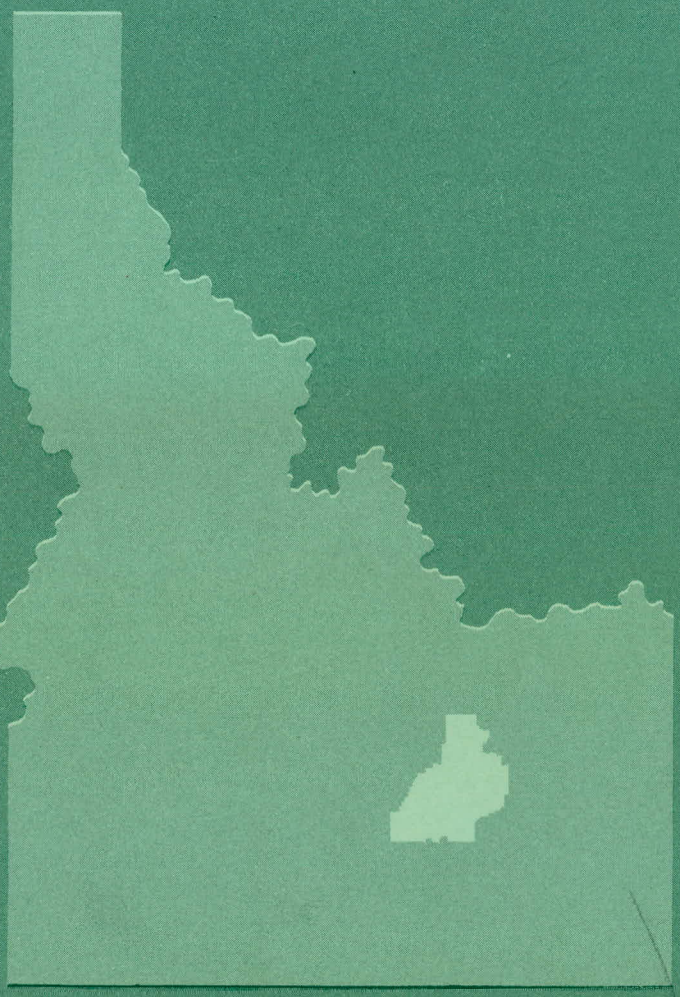

PHILLIPS PETROLEUM COMPANY

ATOMIC ENERGY DIVISION

NATIONAL REACTOR TESTING STATION

US ATOMIC ENERGY COMMISSION

DISCLAIMER

This report was prepared as an account of work sponsored by an agency of the United States Government. Neither the United States Government nor any agency Thereof, nor any of their employees, makes any warranty, express or implied, or assumes any legal liability or responsibility for the accuracy, completeness, or usefulness of any information, apparatus, product, or process disclosed, or represents that its use would not infringe privately owned rights. Reference herein to any specific commercial product, process, or service by trade name, trademark, manufacturer, or otherwise does not necessarily constitute or imply its endorsement, recommendation, or favoring by the United States Government or any agency thereof. The views and opinions of authors expressed herein do not necessarily state or reflect those of the United States Government or any agency thereof.

DISCLAIMER

Portions of this document may be illegible in electronic image products. Images are produced from the best available original document.

PRICE $1.00

Available from the
Office of Technical Services
U. S. Department of Commerce
Washington 25, D. C.

LEGAL NOTICE

This report was prepared as an account of Government sponsored work. Neither the United States, nor the Commission, nor any person acting on behalf of the Commission:

A. Makes any warranty or representation, express or implied, with respect to the accuracy, completeness, or usefulness of the information contained in this report, or that the use of any information, apparatus, method, or process disclosed in this report may not infringe privately owned rights; or

B. Assumes any liabilities with respect to the use of, or for damages resulting from the use of any information, apparatus, method, or process disclosed in this report.

As used in the above, "person acting on behalf of the Commission" includes any employee or contractor of the Commission, or employee of such contractor, to the extent that such employee or contractor of the Commission, or employee of such contractor prepares, disseminates, or provides access to, any information pursuant to his employment or contract with the Commission, or his employment with such contractor.

Printed in USA

IDO-14621
AEC Research & Development Report
General, Miscellaneous, and Progress Reports
TID-4500 (25th Ed.)
Issued: January 15, 1964

CHEMICAL PROCESSING TECHNOLOGY
QUARTERLY PROGRESS REPORT

April - June, 1963

J. R. Huffman
Assistant Manager, Technical

J. A. McBride
Manager, Chemical Technology

J. R. Bower
Editor

PHILLIPS
PETROLEUM
COMPANY

Atomic Energy Division
Contract AT(10-1)-205
Idaho Operations Office
U. S. ATOMIC ENERGY COMMISSION

ICPP Quarterly Reports

1959

Quarter	Number
1	IDO-14471
2	IDO-14494
3	IDO-14509
4	IDO-14512

1960

Quarter	Number
1	IDO-14520
2	IDO-14534
3	IDO-14540
4	IDO-14553

1961

Quarter	Number
1	IDO-14560
2	IDO-14567
3	IDO-14574
4	IDO-14583

1962

Quarter	Number
1	IDO-14589
2	IDO-14593
3	IDO-14599
4	IDO-14611

1963

Quarter	Number
1	IDO-14616

CHEMICAL PROCESSING TECHNOLOGY
QUARTERLY PROGRESS REPORT
APRIL - JUNE, 1963

SUMMARY

ICPP Processing Operations included dissolution and first cycle extraction of all available ETR, MTR, LITR, WTR, and GETR fuel elements; rates averaged 90 percent of capacity, and decontamination factors were normal. Processing capacity of the plant for Brookhaven Graphite Research Reactor (BGRR) fuel was limited due to the element shape and low uranium loading. A facility capable of flattening these elements to 1/3 of the original bulk, without an excessive release of fission products to the basin, was designed and tested successfully. Favorable laboratory results have been obtained in processing OMRE fuel without prior removal of the coating of degraded organic coolant.

Zirconium Fuel Processing Studies demonstrated a significantly higher dissolution rate for the meat of irradiated PWR-type fuel than for the cladding, indicating that accumulation of undissolved uranium in the dissolver would be unlikely during plant operation. Boiling 0.1M chromic acid was effective in removing solids containing uranium fluoride generated adjacent to reagent nozzles in a Monel zirconium-process dissolver.

Dibutyl Phosphate, a TBP degradation product encountered in uranium extraction processes, was removed from first cycle product by adsorption on hydrated zirconia under a variety of laboratory and pilot plant conditions; the loaded zirconia bed was readily regenerated with sodium hydroxide without adverse effects on continued use. A new dibutyl phosphate complex, $[UO_2(NO_3)(DBP)\cdot TBP]_x$, indicated by correlation of previously published data with newer ICPP process data, offers the possibility of describing the distribution of uranium and DBP species during the back extraction operation.

Electrolytic Dissolver anode current densities of 3.2 amps/cm^2 have been achieved in a pilot unit utilizing a dissolver solution of 6.5M nitric acid containing less than 20 g of dissolved stainless steel per liter; a current density of 2.1 amps/cm^2 was achieved in solutions containing 50 to 70 g/l of dissolved stainless steel. The main limitation in achieving higher current densities was believed to be anode polarization and the accompanying gassing; temperature and solution gap were important, principally as they influenced the gas evolution and confinement.

Waste Treatment Studies, directed at adsorption of radioactive cerium and chromium from MTR pond wastes by natural earth materials, indicated that the presence of EDTA had little influence on the distribution coefficient of 1000 when the elements were present as cations. With chromium as a dichromate rather than as a cation, the nature of the adsorbent became significant; lignite maintained its efficiency, due to its combination of anion and cation exchange properties, while clay and clinoptilolite lost efficiency due to the lack of anion exchange properties. Extensive improvements in the aluminum nitrate freeze-melt apparatus for separation of fission products from first cycle aluminum-process raffinates also are discussed.

The ICPP Waste Calcining Facility is being readied for production operation with ICPP stored wastes. Results of laboratory and pilot plant studies on mercury retention, calcine particle growth, fines generation, and possible incorporation of calcine in solid matrices are summarized.

Plant Improvement Studies reported include initial hot runs on a steam stripper for removal of plutonium from TBP-Amsco; alpha activity was reduced from 10^4 counts/minute to background. New cadmium-poisoned fuel storage racks were designed to give more efficient utilization of basin storage space through closer spacing of the stored elements.

CHEMICAL PROCESSING TECHNOLOGY
QUARTERLY PROGRESS REPORT
APRIL - JUNE, 1963

CONTENTS

SUMMARY iii

I. ICPP OPERATIONAL SCHEDULE, PERFORMANCE, AND PROBLEMS 1

1. ICPP OPERATIONS 1

2. PLANT ASSISTANCE PROBLEMS 1

2.1 BGRR Fuel Processing 1
2.2 Demonstration of BGRR Fuel Element Flattening. 1
2.3 OMRE Fuel Processing Studies 5
2.4 Corrosion of Boron Stainless Steel 6

II. AQUEOUS PROCESS STUDIES 8

1. AQUEOUS ZIRCONIUM FUEL PROCESSING 8

1.1 Relative Rates of Dissolution for Meat and Cladding of Irradiated Uranium-Zirconium Alloy Fuels 8
1.2 Removal of Uranium Solids from Monel Surfaces 8

2. TRIBUTYL PHOSPHATE DEGRADATION STUDIES 10

2.1 Laboratory Studies of Dibutyl Phosphate Adsorption on Zirconia 10
2.2 Pilot Plant Study of Dibutyl Phosphate Adsorption on Zirconia 12
2.3 Dibutyl Phosphate Chemistry 12

III. ELECTROLYTIC DISSOLUTION SYSTEMS 14

1. ELECTROLYTIC DISSOLUTION - PILOT PLANT STUDIES 14

1.1 General Performance Results 14
1.2 Voltage Probe Measurements of Polarization 15
1.3 Stainless Steel Limiting Current Densities 17

IV. NEW WASTE TREATMENT METHODS 19

1. DISPOSAL OF LOW-LEVEL RADIOACTIVE WASTES 19

2. DECONTAMINATION OF ALUMINUM NITRATE BY THE FREEZE-MELT TECHNIQUE 19

V. WASTE CALCINATION 22

1. MODIFICATION OF THE WASTE CALCINING FACILITY (WCF) 22

2. PILOT PLANT DEVELOPMENT STUDIES 22

2.1 Pilot Plant Calciner Operation 22
2.2 Vessel Sparge Test 22

3. BEHAVIOR OF MERCURY IN FLUIDIZED BED CALCINATION . . 23

4. STUDIES OF CALCINATION MECHANISMS 23

4.1 Particle Growth Rate Studies 23
4.2 Mechanism of Fines Generation 25

5. STORAGE OF CALCINED ALUMINA 29

VI. PLANT IMPROVEMENTS 31

1. PLANT INSTRUMENTATION 31

2. WASTE SOLVENT CLEANUP FACILITY 31

3. NUCLEAR POISONED FUEL STORAGE RACKS 32

VII. REPORTS AND PUBLICATIONS ISSUED DURING THE QUARTER . . . 33

VIII. REFERENCES 34

FIGURES

1. Hydraulic press and two BGRR fuel elements in multicurie cell 2

2. BGRR fuel elements after storage in FECF basin for several months . . 2

3. Two BGRR fuel elements - left, unflattened; right, after 800 psig in . . . 3
press

4. Four BGRR fuel elements, two flattened at 1500 psig and two unflattened 4

5. Adsorption of dibutyl phosphate on zirconium oxide (Column 1). 10

6. Adsorption of dibutyl phosphate on zirconium oxide (Column 2). 11

7. Adsorption of dibutyl phosphate on zirconium oxide (Column 3). 11

8. Potential-current diagram (Series I) 15

9. Potential-current diagram (Series II) 16

10. Potential-current diagram (Series III) 16

11. Potential-current diagram (Series IV) 16

12. Potential-current diagram (Series V) 16

13. Variation of current with available stainless steel area for shaped charge at 15 volts 17

14. Schematic diagram of freeze-melt tray and heat transfer system 20

15. Effect of calcination temperature on the retention of mercury in calciner product 23

16. Photomicrograph of sectioned calciner product particles showing growth rings 25

17. Comparison of experimental fines generation data with computer solution of mathematic derived fines generation model 28

TABLES

I. Settling Data for Corrosion Product Solids 5

II. Concentration of Radioisotopes in Corrosion Product Solids from BGRR Fuel Elements 5

III. Corrosion Measurements of Boron Stainless Steel 6

IV. Reagents Tested for Removal of Uranium Solids Adherent to Monel Surfaces 9

V. Behavior of Mercury in Two-Foot-Square Calciner and Venturi Scrubber 24

VI. Common Calciner Operation Conditions for Tests of Model of Mechanism of Fines Generation 27

VII. Summary of Unique Experimental Operating Conditions and Results for Tests of the Model of Mechanism of Fines Generation 27

VIII. Wettability of Calcined Alumina with Various Materials 30

I. ICPP OPERATIONAL SCHEDULE, PERFORMANCE, AND PROBLEMS

1. ICPP OPERATIONS

The ICPP processed irradiated aluminum fuels through the first cycle during this period. Most of the inventory of ETR, MTR, LITR, WTR, and GETR fuels was processed prior to June 30.

Plant operation was quite satisfactory with throughput averaging about 90 percent of capacity. Preliminary decontamination factors for the first cycle, from four sets of samples, were as follows: log beta, between 2.7 and 3.8; log gamma, between 1.0 and 2.8. These decontamination factors are consistent with those obtained from previous runs. Samples which will permit further study of decontamination factors and determination of phosphorous distribution in various streams were taken and are being analyzed.

2. PLANT ASSISTANCE PROBLEMS

2.1 BGRR Fuel Processing (M. E. Weech, Problem Leader; P. Burn)

The fuel storage basin contains approximately 3000 Brookhaven Graphite Research Reactor (BGRR) fuel assemblies which are too bulky to transport to the CPM dissolvers in the conventional manner at an economical rate. Studies have shown that flattening these elements would permit handling at an economical rate. Flattening tests, discussed in Section 2.2, showed these assemblies could be compressed to approximately 1/3 of their original volume in a ten-ton press without element fragmentation or appreciable cracking. An underwater facility was designed to flatten the entire lot before processing. The corrosion scale which flakes during flattening will be collected and buried. The release of soluble activity to the basin water should be negligible.

2.2 Demonstration of BGRR Fuel Element Flattening (D. W. Rhodes, Problem Leader; L. A. Decker, M. E. Jacobson, M. W. Wilding, B. J. Newby)

Irradiated fuel elements from the Brookhaven Graphite Research Reactor (BGRR) are stored in the ICPP Fuel Storage Facility prior to reprocessing. These fuel element assemblies are fabricated from fuel plates, each 2.25 inches wide x 24 inches long x 0.06 to 0.08 inch thick and containing, after irradiation, about three grams of U-235 imbedded in an aluminum matrix and clad with aluminum. These plates are bent along the axis of the long dimension into a 60° angle and three such bent plates are formed into an element by welding the ends to a ring (see Figures 1 through 4). The large packing volume to weight ratio of these fuel elements, together with the low uranium content, makes utilization of storage basin space relatively inefficient. These factors also make it impossible, with present equipment, to transport the elements from storage to the processing dissolver fast enough to keep the dissolver operating at its design capacity. As a possible solution to the problem, a test was devised to flatten the elements, thus reducing the packing volume-to-weight ratio to a satisfactory value.

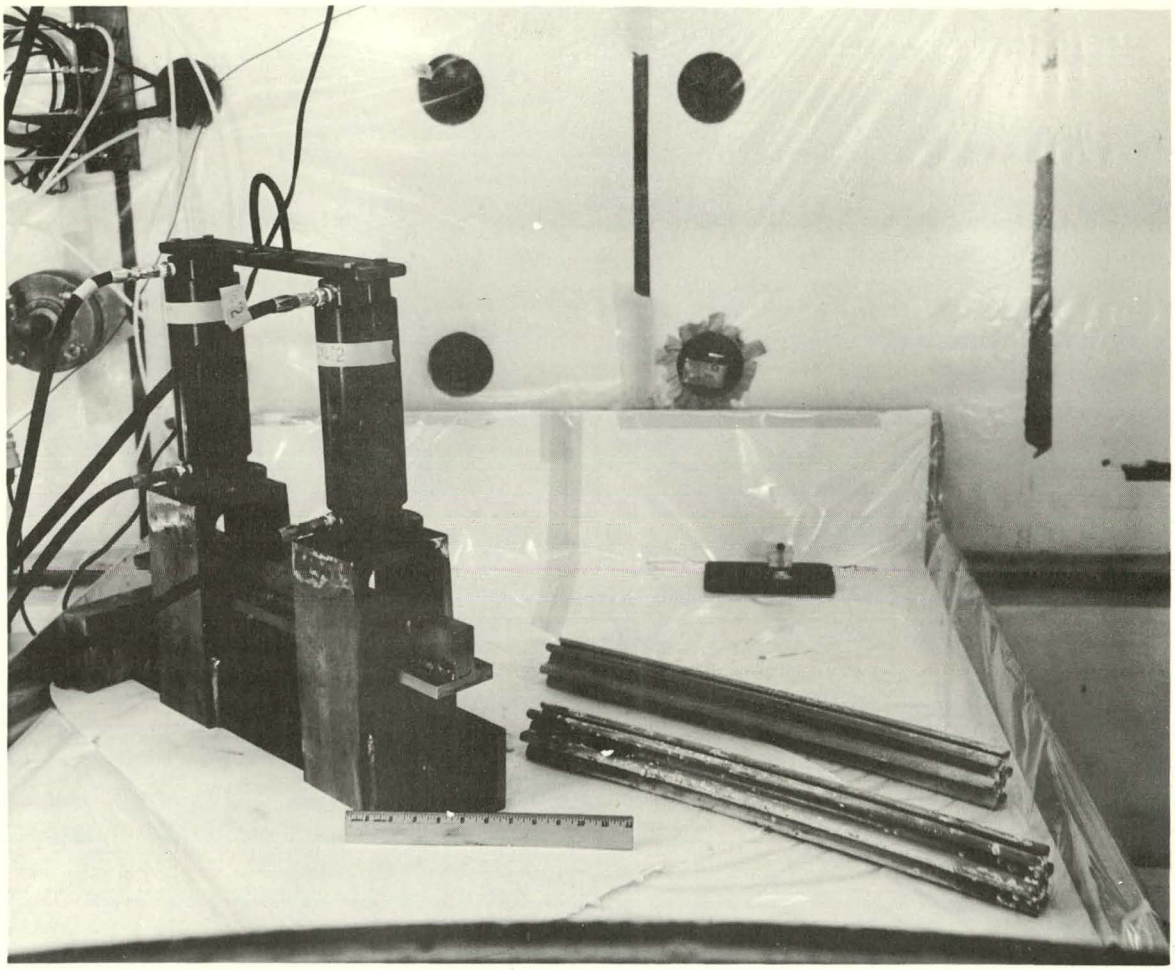

Fig. 1 Hydraulic press and two BGRR fuel elements in multicurie cell.

2.21 Mechanical Testing. A simple hydraulic press, shown in Figure 1, was devised to flatten the BGRR fuel elements in the ICPP Multicurie Cell. The double acting hydraulic cylinders have a bore of three inches and, with 1500 psig hydraulic pressure, develop a force of 10,603 pounds each. This hydraulic pressure was used in each case except as noted. Observations were made of the thickness of the element at various stages in the flattening, as well as the condition of the surface to detect evidences of cladding failure, either before or during flattening.

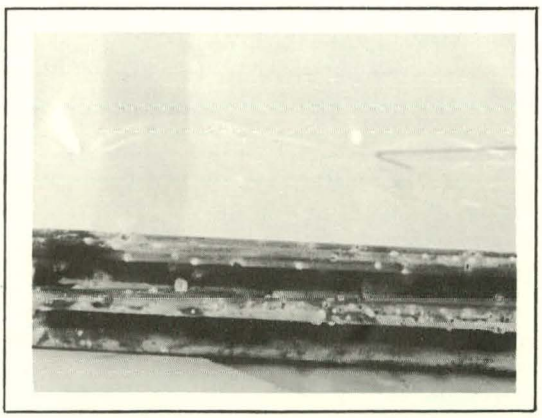

Fig. 2 BGRR fuel elements after storage in FECF basin for several months.

The first element tested was subjected to several different pressure tests. First, 400-psig hydraulic pressure was applied to the system. The plates of the element did not bend at all, but the connecting rings at each end did.

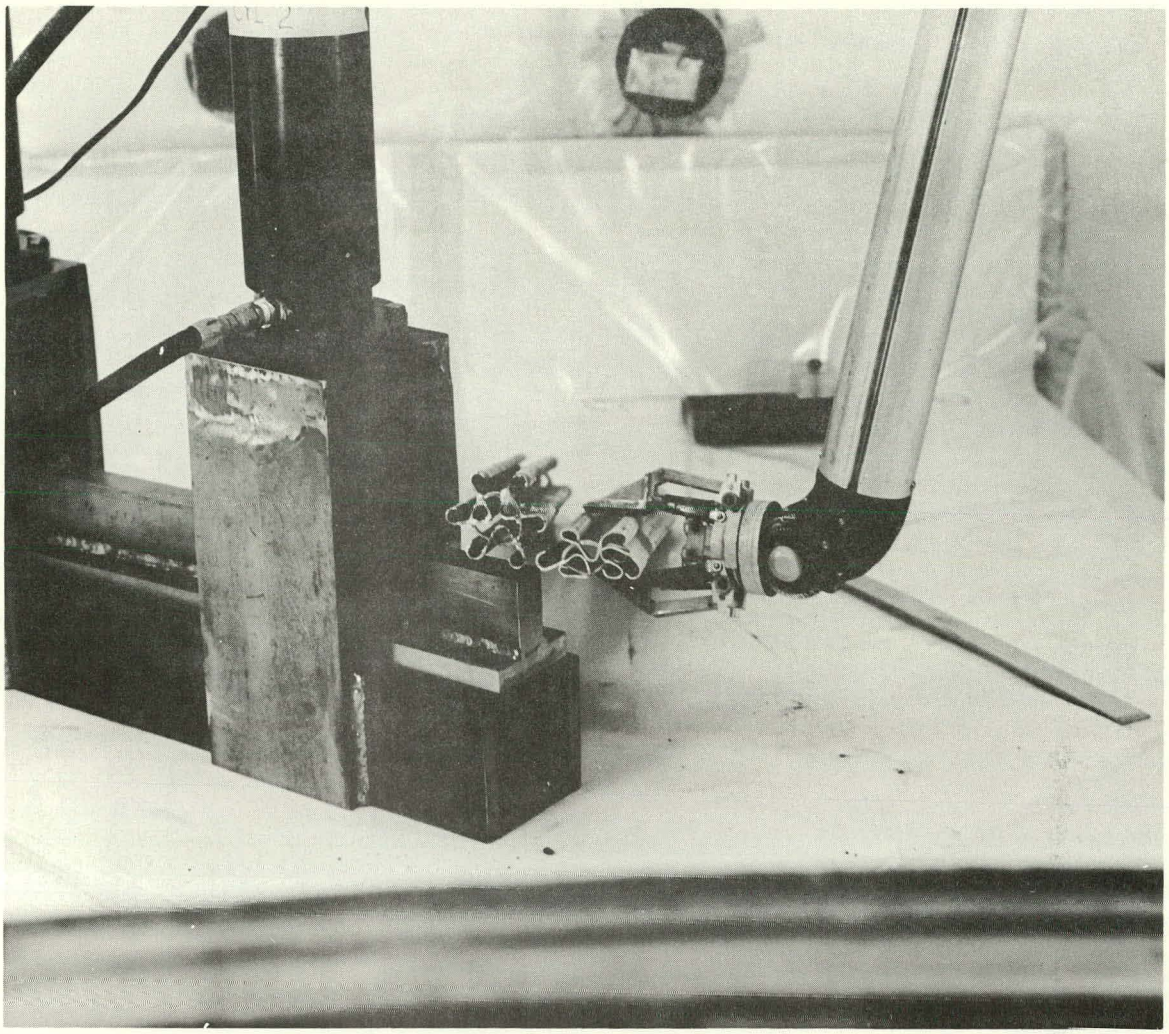

Fig. 3 Two BGRR fuel elements - left, unflattened; right, after 800 psig in press.

Increasing the pressure to 800 psig flattened the element to about 1/2 its original diameter as shown in Figure 3 (right). A hydraulic pressure of 1500 psig flattened the elements to about 3/4-inch (Figure 4).

In all, nine fuel elements were flattened in these tests in the Multicurie Cell hydraulic press. Visual inspection with short-range, wide-vision binoculars indicated that no shattering occurred; however, one element showed evidence of cracks along the rolled edge.

2.22 Corrosion Product Contamination. In the course of handling BGRR fuel elements that had been stored in the basin for several months, solid deposits were observed on the surface of the fuel. Further investigation indicated that the fuel element surfaces corrode rapidly under the present conditions of storage in the basin water, ie, stacked horizontally in a tray. This corrosion results in penetration of the cladding and a subsequent buildup of solid corrosion products around these points of penetration with some release of fission

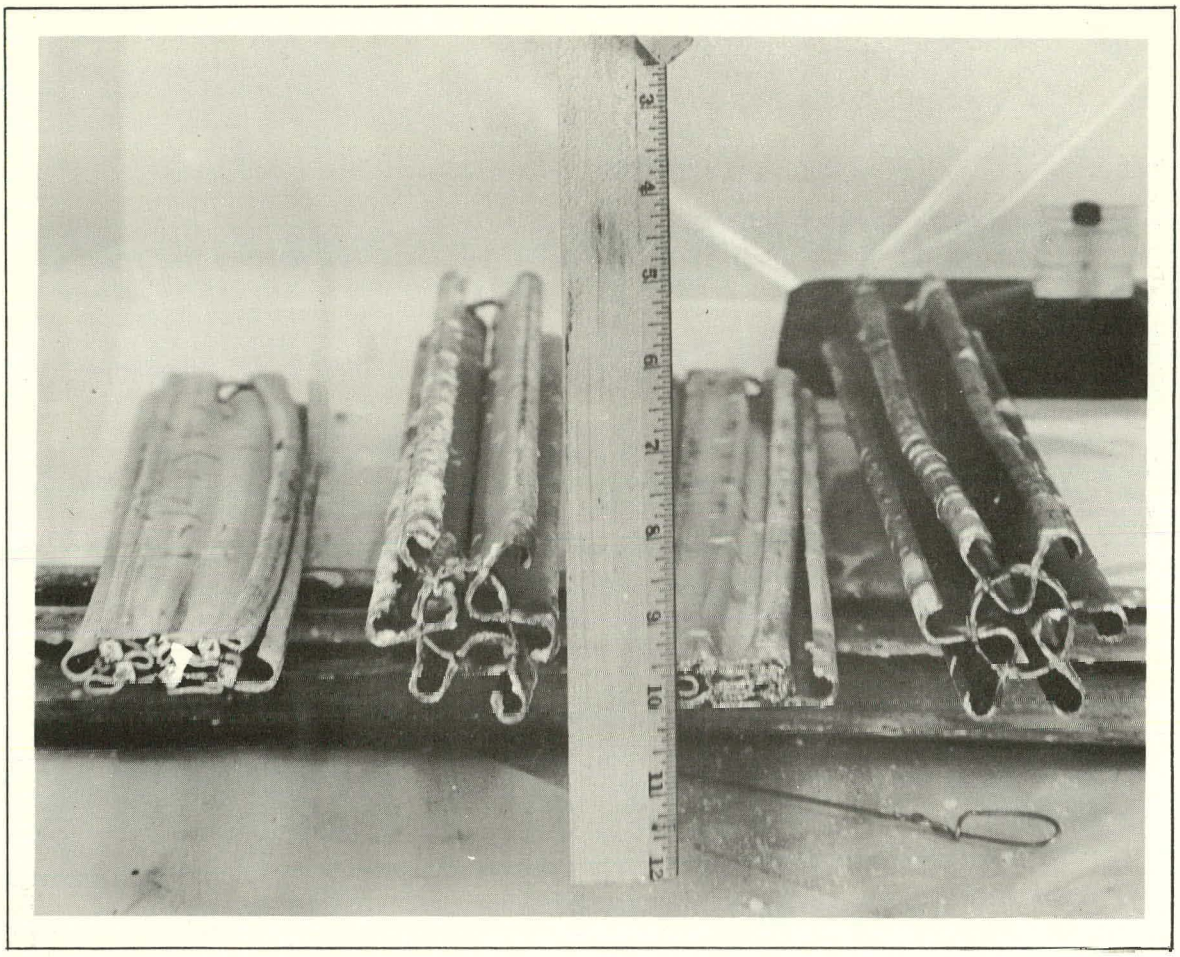

Fig. 4 Four BGRR fuel elements, two flattened at 1500 psig and two unflattened.

products and uranium to the water. The corrosion product "blisters", which by X-ray diffraction and chemical analysis appear to be amorphous aluminosilicates, can be seen in Figure 2 on the surfaces of the fuel.

To determine the amount and nature of the solids dislodged from the fuel elements during flattening, all of the corrosion product solids that were dislodged by flattening one fuel element were collected in water. After thoroughly stirring the suspension in a filled two-gallon bottle, aliquots were removed periodically from a 10 cm depth by pipetting. These samples were used to determine the amount of solids remaining in suspension after a given settling time. The results are shown in Table I.

Weight measurements indicated that about five grams of solid would be released from each fuel element that was flattened. Radiochemical analyses of the corrosion product solids from six different trays in the storage basin are shown in Table II.

The results in Table II indicate that the specific activity of the solids is about one millicurie per gram of solid. Thus, the 3000 BGRR fuel elements in storage would release, when flattened in the press, about 15 kg of solids containing approximately 15 curies of fission products. Since the bulk of the

TABLE I

SETTLING DATA FOR CORROSION PRODUCT SOLIDS

Settling Time	Percent of Solids Settled Past 10 cm Depth
3.25 min	91.6
7.5 min	93.7
15 min	96.4
30 min	97.7
1 hr	98.3
2 hr	98.2
20 hr	98.5

TABLE II

CONCENTRATION OF RADIOISOTOPES IN CORROSION PRODUCT SOLIDS FROM BGRR FUEL ELEMENTS

Sample No.	Cs-137 d/(min)(g)	Sr-90 d/(min)(g)	Ce-144 d/(min)(g)	Ru-106 d/(min)(g)	U g/g	Total β d/(min)(g)	Total γ c/(min)(g)
1	3.1×10^6	3.1×10^7	5.8×10^8	2.3×10^7	0.0152	1.4×10^9	4.5×10^7
2	2.6×10^6	3.8×10^7	8.3×10^7	4.6×10^7	0.0151	1.9×10^9	6.9×10^7
3	6.2×10^6	7.9×10^7	56.4×10^8	39.7×10^7	0.0120	10.8×10^9	40.0×10^7
4	13.6×10^6	5.4×10^7	9.4×10^8	9.6×10^7	0.0176	2.4×10^9	8.8×10^7
5	2.0×10^6	3.0×10^7	3.9×10^8	1.2×10^7	0.0142	1.0×10^9	3.4×10^7
6	32.0×10^6	23.3×10^7	28.4×10^8	11.7×10^7	--	11.7×10^9	29.3×10^7
Average	15.8×10^6	10.8×10^7	18.7×10^8	11.5×10^7	--	4.9×10^9	15.5×10^7

Cs-137 + Sr-90 + Ce-144 + Ru-106 = 2.1×109 d/(min)(g) $\approx$ 1 mc/g

solids can be collected during the flattening process, the probability of serious contamination of the storage basin water by these solids is low; for comparison purposes, the average total amount of fission products in solution in the storage basins (1,500,000 gallons of water) has been in the range 10 to 15 curies for the past several months.

Five of the flattened elements, including the one with possible cracks, were placed in a sealed container containing fresh water. The water was then sampled periodically to measure the buildup of radioactive isotopes. The results indicated that no more fission products were leached from these flattened elements than from silimar elements which had not been altered in any way. Apparently, these elements can be flattened and stored in the basin for at least a few weeks without an excessive release of fission products to the basin water.

2.3 OMRE Fuel Processing Studies (K. L. Rohde, Problem Leader; L. A. Decker, M. E. Jacobson)

The ICPP has two cores from the Organic Moderated Reactor Experiment (OMRE) remaining to be reprocessed. The fuel elements from the OMRE are

coated with a carbonaceous film from the degradation products of the organic moderator fluid. The first core from this reactor was processed several years ago [1] by first attempting to remove this film with Turco 4502 followed by dissolution in sulfuric acid. Recent experiments on dissolution of these coated fuel plates showed that it may be possible to process the fuel elements without treatment to remove the film coating.

Dissolution of the untreated, coated fuel was carried out both in 6.5M sulfuric acid and electrolytically in 8M nitric acid. There was no detectable difference in rates of dissolution compared with those obtained under similar conditions for treated (coating removed) fuel.

A pulsed extraction column was operated with feed solution obtained from dissolution of fuel samples in 6.5M sulfuric acid. The column performed as it had in cold operation with simulated feed. Future work will involve operation of the pulsed column with feed obtained from electrolytic dissolution of the irradiated, coated fuel.

2.4 Corrosion of Boron Stainless Steel (T. L. Hoffman)

Laboratory tests (ASTM A 262-55T) using boiling 65 percent nitric acid were conducted on coupons of plate rolled from nine different billets of Type 304 stainless steel containing about 1.5 percent boron. This stainless steel is being used in some ICPP process vessels as poisoned grids for criticality safeguard. The average corrosion rates based on weight measurements on coupons from the nine billets were 9.3 and 10.1 mils per month for unwelded and welded coupons, respectively; this is a fourfold increase over the rates for boron-free Type 304 stainless steel predictable from the manufacturer's corrosion data. Iron, chromium, boron, and nickel were dissolving, apparently from the grain boundaries of the alloy. There was no selective dissolution of boron. Table III

TABLE III

CORROSION MEASUREMENTS OF BORON STAINLESS STEEL

	Penetration, In/Mo (Based on Weight Loss)					
	First 48 Hours		Second 48 Hours		Third 48 Hours	
Billet No.	Unwelded	Welded	Unwelded	Welded	Unwelded	Welded
0-16273	0.0060	0.0069	0.0097	0.0168	0.0097	0.0101
0-16274	0.0061	0.0065	0.0094	0.0162	0.0065	0.0076
0-16275	0.0074	0.0074	0.0113	0.0114	0.0089	0.0098
0-16276	0.0083	0.0077	0.0085	0.0080	0.0088	0.0087
0-16277	0.0094	0.0090	0.0099	0.0096	0.0112	0.0113
0-16278	0.0092	0.0104	0.0072	0.0092	0.0144	0.0182
0-16280	0.0083	0.0085	0.0097	0.0099	0.0095	0.0105
0 16281	0.0095	0.0087	0.0108	0.0095	0.0115	0.0104
0-16368	0.0084	0.0086	0.0111	0.0108	0.0102	0.0105

lists the results of these tests. A standard analysis of variance test performed on these results indicated that all nine billets have the same corrosion properties.

The poisoned grids in a continuous product evaporator and in four product storage vessels were fabricated from randomly selected plates which were rolled from the nine different billets. Plates from three additional billets (not laboratory tested) also were used in the grid for one of the four storage vessels.

For the purpose of in-plant surveillance, coupons representing each of the nine tested billets were installed in the continuous product evaporator and four product storage vessels so as to have pairs of coupons representing three billets in each vessel. In addition, coupons from three billets which had not been laboratory tested were inserted in the storage vessel containing grids of these materials. All coupons inserted in the plant vessels will be removed periodically for corrosion evaluation.

II. AQUEOUS PROCESS STUDIES

(Section Chiefs: K. L. Rohde, Chemistry; J. A. Buckham, Development Engineering)

1. AQUEOUS ZIRCONIUM FUEL PROCESSING

1.1 Relative Rates of Dissolution for Meat and Cladding of Irradiated Uranium-Zirconium Alloy Fuels (K. L. Rohde, Problem Leader; L. A. Decker, M. E. Jacobson)

In order to assure safe operation of a continuous dissolver for processing PWR-type uranium-zirconium alloy fuels, it was necessary to determine that there would be no great accumulation of uranium-235 in the dissolver during extended operation. Such an accumulation could occur if the uranium-containing meat alloy were to dissolve at an appreciably slower rate than the cladding alloy.

The relative rates of dissolution for meat and cladding alloys were determined in the usual dissolvent, 5.2M hydrofluoric acid, 0.34M boric acid, and 0.03M nitric acid. Duplicate determinations were made for both unirradiated fuel and fuel having greater than 50 percent burnup. From these determinations, an estimate was made of the absolute dissolution rates for meat and cladding alloys. At about 95°C (with an insignificant amount of zirconium dissolved) the approximate initial dissolution rates were:

Unirradiated: cladding - 80 mg/(cm^2)(min); meat - 160 mg/(cm^2)(min)

Irradiated: cladding - 25 mg/(cm^2)(min); meat - 500 mg/(cm^2)(min)

The ratio of the rate of dissolution of cladding to the rate of dissolution of meat was about 0.5 for the unirradiated fuel and about 0.05 for the irradiated fuel. Therefore, it was concluded that the meat material will dissolve essentially as rapidly as it is exposed by the dissolution of the cladding and that there will be no accumulation of uranium in the dissolver.

1.2 Removal of Uranium Solids from Monel Surfaces (D. W. Rhodes, Problem Leader; B. J. Newby, B. E. Paige)

Studies were made to investigate the removal from Monel surfaces of uranium-containing solids, presumably fluorides, which adhere to dissolver surfaces during continuous dissolution of uranium-zirconium alloy fuel. A reagent was desired that would effectively remove uranium solids from Monel surfaces, yet be relatively noncorrosive to Monel.

Reagents known to dissolve uranium compounds or form soluble uranium complexes were studied. Some of the work was done using Monel coupons having approximately three square inches of surface area that had been coated with uranium solids during continuous dissolution of uranium-Zircaloy-2 fuel pieces; in other experiments, sections of about 2.5 square inches were cut from 1/2-inch (inside diameter) continuous dissolvers that had become coated with uranium solids during operation. To utilize better the Monel samples that were coated with uranium solids, the same piece was sometimes used to test the effectiveness of a number of treatments. The quantity of uranium solid that was deposited on a given surface area varied widely, and thus tended to complicate interpretation of the results. The coated sample (along

with a welded Monel corrosion coupon in many experiments) was suspended in a given volume of the reagent to be tested, the solution was stirred, and small aliquots of solution were removed at intervals to indicate how rapidly the uranium was removed.

The reagents and conditions tested for removing uranium fluoride solids from Monel surfaces are listed in decreasing order of effectiveness in Table IV. Boiling 0.1M chromic acid was by far the most effective. For example, 200 ml of boiling 0.1M chromic acid removed all of the uranium (3.4 g) from 2.5 square inches of surface area in two hours, a performance more than adequate to remove anticipated localized coatings in a plant-scale dissolver. The measured corrosion rate on a welded Monel coupon in this system was about 2.5 mils per month. In addition to its "cleanout" properties and low corrosion rate, this reagent is compatible with the solvent extraction process used at the ICPP. The treatments and conditions listed in the second portion of Table IV are not recommended because of poor efficiency or corrosion properties.

TABLE IV

REAGENTS TESTED FOR REMOVAL OF URANIUM SOLIDS ADHERENT TO MONEL SURFACES

Treatments	Contact Time (hrs)	Temperature (°C)
Part I Potentially Satisfactory Methods for Dissolver Clean-Out		
Chromic acid, 0.1 M	2	95
Ammonium oxalate, 4 percent	4	95
Sodium hydroxide, 0.5, 2, and 5 M, and sodium peroxide, 0.1, 0.2, 0.3, and 0.4 M	4	25
Sodium hydroxide, 20 percent, and metallic zinc	1	95
Hydrofluoric acid, 28 M, followed by 0.1, 0.3, and 2.2 M aluminum nitrate	4 + 1	95
Aluminum nitrate, 0.1, 0.5, and 2.2 M	4	25
Part II Unsatisfactory Methods		
Nitric acid, 0.1, 0.3, 0.5, and 1 M	1	95
Hydrofluoric acid, 4.8 M, and nitric acid, 0.3 M	1	95
Hydrofluoric acid, 28 M, followed by 0.3 M nitric acid	4 + 1	95
Nitric acid, 1 M, and boric acid, 0.2 M	1	95
Hydrofluoric acid, 28 M, followed by 0.5 M hydrogen peroxide	4 + 1	95 - 60
Sodium carbonate, 1.8 M, and sodium peroxide, 0.1 M	4	60
Ammonium hydroxide, 0.5 and 5.0 M, and hydrogen peroxide, 0.01 and 0.1 M	1	25
Hydrofluoric acid, 1, 5, and 28 M	4	95
Dilute ziroconium hydrofluoric acid dissolver solution	4	95

2. TRIBUTYL PHOSPHATE DEGRADATION STUDIES

2.1 Laboratory Studies of Dibutyl Phosphate Adsorption on Zirconia (H. T. Hahn, Problem Leader; R. G. Butzman)

The laboratory experimental program [2] concerned with the removal of TBP degradation products from the ICPP first cycle mixer-settler product, using an inorganic ion-exchanger, is now nearly complete. The inorganic exchange material used was hydrated zirconia, Bio-Rad HZO-1. The program consisted of three separate column loading experiments; the first with -40+60 mesh zirconia, and the other two with -20+40 mesh zirconia.

The first column experiment, which was started last quarter, continued for 61 days. In order to observe the effects of flow rate, the column flow was altered several times. Flow rates used (chronologically) were 1.2, 1.6, 0.6, and 1.6 l/(hr)(lb). The only significant change in performance with changing flow rate resulted when the rate was increased from 0.6 to 1.6 l/(hr)(lb); this resulted in a small but sharp drop in DF (Figure 5). Initially, it was planned to completely load the column, but the approach to saturation became too gradual. The total amount of HDBP taken up by this column was approximately 0.174 meq/g of exchanger.

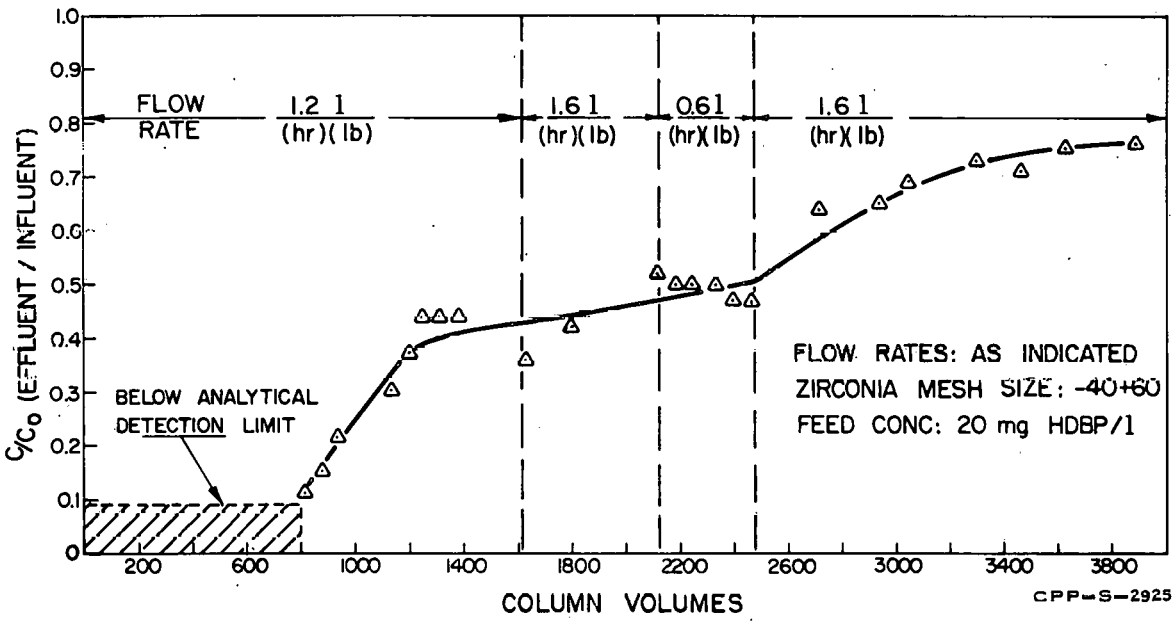

Fig. 5 Adsorption of dibutyl phosphate on zirconium oxide (Column 1).

The second column experiment was conducted over a 49-day period using 2.26 g of -20+40 mesh NZO-1. The influent concentration was 18-20 mg HDBP/l in 0.04M HZO_3 with 0.02M UNH present. The flow rate for this column was held constant at 1.2 l/(hr)(lb). The total amount of HDBP sorbed on the exchanger was 0.159 meq/g at 2940 column volumes. The approach to saturation (Figure 6) began to level in much the same way as it did in the first experiment.

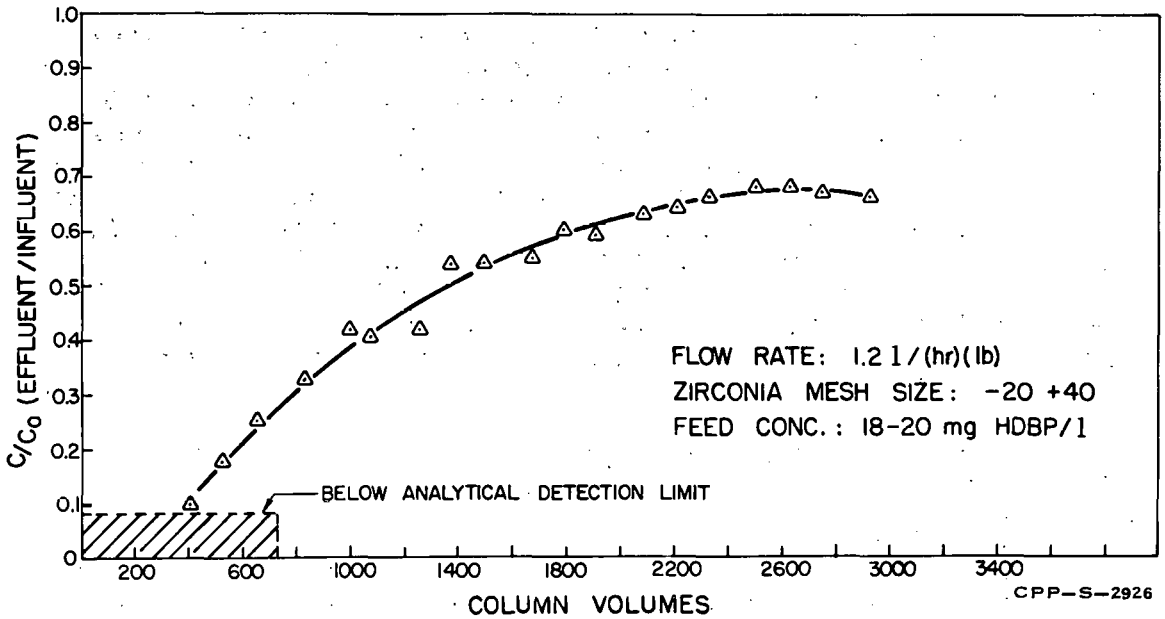

Fig. 6 Adsorption of dibutyl phosphate on zirconium oxide (Column 2).

A third column experiment was conducted for the purpose of observing the sorptive behavior of HDBP from an influent of low concentration; ie, approximately 1.0 mg/l as opposed to 20 mg/l. Again, the bed consisted of 2.26 g of -20+40 mesh HZO-1 and the feed contained 0.04M HNO_3, 0.02M UNH, and 1 mg HDBP/l. The column was operated at a constant flow of 1.0 l/(hr)(lb) for 50 days (Figure 7), and at the close of the run, contained only 0.0083 meq HDBP/g of exchanger.

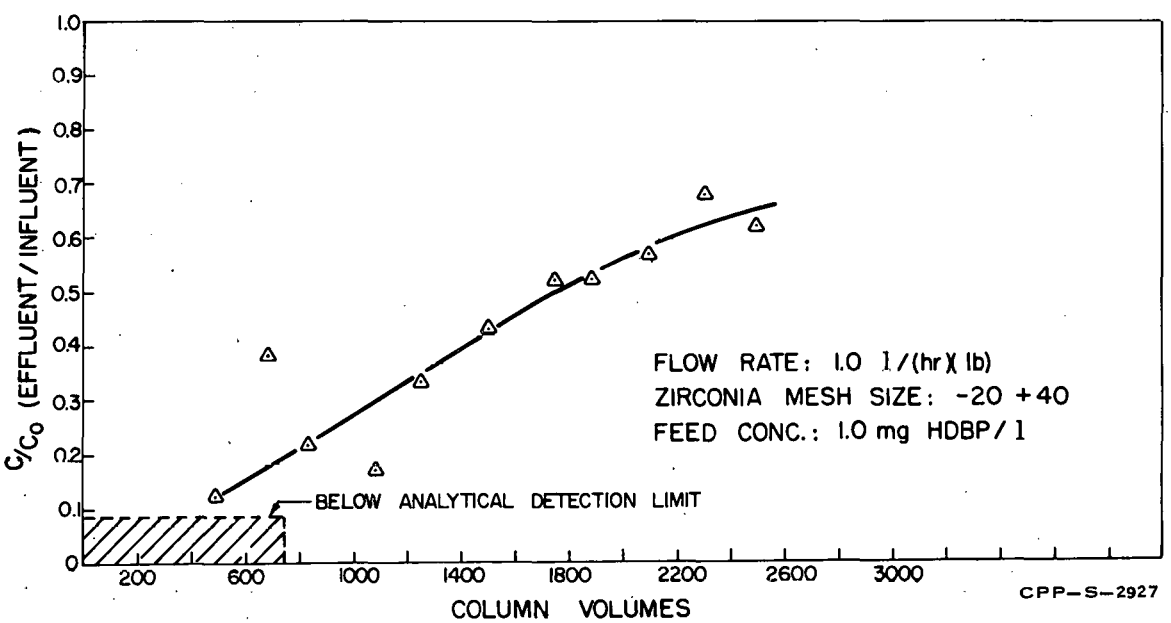

Fig. 7 Adsorption of dibutyl phosphate on zirconium oxide (Column 3).

It was necessary to pretreat the exchanger for the columns with 0.04M HNO_3 to prevent sorption of uranium. Comparing the two particle size ranges, the -40+60 mesh provided a DF of 10 or greater for about 800 column volumes. The -20+40 mesh maintained a DF of greater than 10 for about 400 column volumes in both experiments in which it was employed. The apparent HDBP exchange capacity of the zirconia is related to concentration and flow rate. Previous experiments also indicated it may be as high as 0.5 meq HDBP/g of exchanger in the absence of uranium. The similarity of curves for the last two experiments suggests that the capacity is proportional to the influent concentration of HDBP, a higher concentration providing a greater driving force (at the same flow rate) thereby utilizing more of the inner, less accessible exchange sites.

2.2 Pilot Plant Study of Dibutyl Phosphate Adsorption on Zirconia (B. M. Legler, Problem Leader; E. J. Bailey, R. H. Ray)

Pilot plant equipment was assembled to investigate two phases of the adsorption of dibutyl phosphate on a zirconia bed: (a) the effect of regenerating the bed with a sodium hydroxide solution, and (b) the effect of using a bed 100 times larger than the bed used in the original laboratory investigations [3]. A series of ten cycles of dibutyl phosphate adsorption on and regeneration of the zirconia bed was initiated. After six of the intended ten cycles were completed, analytical results gave no indication of adverse effects attributable to regeneration. A cursory review of the data indicates that the larger bed used in the pilot plant may have slightly better performance than the smaller bed used in the laboratory. A more detailed report will be forthcoming on completion of the programmed investigation.

2.3 Dibutyl Phosphate Chemistry (H. T. Hahn, Problem Leader; E. M. Vander Wall)

The interactions of tributyl phosphate (TBP) and its principal decomposition product, dibutyl phosphoric acid (HDBP), with uranyl nitrate and nitric acid are of considerable importance in the reprocessing of nuclear fuels. The phosphoryl complexes exert a synergistic effect on the extraction and retention of uranium and also complex other cations. The resultant compounds may be interfacially active or precipitate during subsequent evaporation.

Recent literature [4, 5, 6, 7] has described several complexes found in all or part of the two-phase system HDBP-TBP-diluent-UO_2^{++}-H^+. Values for the appropriate equilibrium constants were also included. Application of these values to the uranium reextraction operation (ICPP IC column) represents the simplest point for testing since the concentrations involved are sufficiently low that ionic strength effects are minimal, and the lack of activity coefficients for the complexes is least deleterious.

Correlation of previously published uranium extraction coefficients [8] and more recent data with known chemical concentrations in the IC column system (TBP-Amsco-UNH-HNO_3-HDBP) has shown that the equilibrium constants in the literature [4, 5, 6, 7] do not adequately describe the uranium, HDBP, or nitrate distribution observed. The addition of a new complex, $[UO_2(NO_3)(DBP)\cdot TBP]_x$, to the system yields a reasonable agreement with the experimental data. The best correlation is obtained with $x = 2$, although the complex with $x = 1$ cannot be excluded. The correlation has been programmed for computation on an IBM 7090 computer.

The complex is apparently optically active in the ultraviolet, with six absorption peaks (3075, 3150, 3220, 3295, 3390, 3485 Å) associated with its presence.

A plant sampling program has been undertaken to confirm the presence of HDBP in the first cycle. Preliminary analytical results have shown a minimum of three milligrams DBP^- per liter at all six sampling points. The highest result reported to date has been 133 milligrams DBP^- per liter in the first cycle product.

III. ELECTROLYTIC DISSOLUTION SYSTEMS

(Section Chiefs: K. L. Rohde, Chemistry; M. E. Weech, Plant Processes)

1. ELECTROLYTIC DISSOLUTION - PILOT PLANT STUDIES

(M. E. Weech and H. T. Hahn, Problem Leaders;
R. G. Denney, W. B. Kerr, J. C. Petrie)

Preliminary experiments have been made with the Model 1 solution-contact electrolytic dissolver [9]. Two series of measurements were made under idealized conditions. In one series the potential drops between various points within the dissolver were measured to determine the behavior of system resistances under actual operating conditions. In a second series, the limiting current density of the anodic and cathodic faces of a stainless steel charge were estimated for a product solution of the desired composition.

Scoping studies were made to explore the effects of dissolvent composition, temperature, voltage, circulation of electrolyte, and electrode - fuel charge spacing on the rate of dissolution of stainless steel.

1.1 General Performance Results

A series of runs was completed to explore the effect of dissolvent composition, temperature, voltage, recirculating rate, and width of electrode-fuel charge solution gap on the capacity of the Model 1 pilot plant [a] solution-contact electrolytic dissolver [9]. Both 304 stainless steel pipe and specially shaped elements, which provide the maximum metal surface facing the electrodes, were dissolved. Anode current densities in excess of 3.2 amps/cm^2 at 20 volts were achieved using 6.5M HNO_3 with less than 20 g stainless steel/liter in solution at a dissolvent temperature of 60°C and a dissolvent recirculation rate of 7 l/min. This represents a direct scale-up processing rate for APPR fuel elements of 10 kg U-235/day in a plant-scale dissolver, and is in agreement with anode current densities reported [10] by Savannah River Laboratory in their solution-contact dissolver using 5.5M HNO_3 with less than 20 g stainless steel/liter at 85°C [10]. Using a more practical recirculating dissolvent of 50-70 g stainless steel/liter and 3-4M HNO_3, only 2.1 amps/cm^2 of anode at 20 volts was achieved. This represents a direct scale-up plant capacity of approximately 6 kg U-235/day.

In tests thus far the optimum dissolvent outlet temperature has been 55-60°C. Increasing the temperature above 60°C results in increased gassing at the anode and a corresponding decrease in current. Temperature measurements in the anode region disclosed no temperature regions approaching the boiling point; therefore, the gassing effects are not attributed to steam generation.

Within the tested range of dissolvent recirculation rate of 0-7 liters per minute, and under the limitations of the present design, no effect has been noted on the current due to recirculation. The dissolver and auxiliary systems are being modified to permit increasing the recirculation rate to 30 liters per minute to study the effect over a wider range.

---

[a] This pilot model dissolver is full-size in cross section but only 1/24 the length of the proposed plant scale dissolver.

A 1/4-inch solution gap between the electrodes and the charge gave only marginal superiority over the 1/2-inch gap in comparison tests at 15 volts, 50-60 g stainless steel/liter, 3-4M HNO_3, 7 liters/min dissolvent recirculation rate, and varying temperatures. Again the anode gap appeared to be limiting. The decreased gap apparently confined the gases and increased the polarization resistance, offsetting the reduced resistance of the liquid gaps.

A modified dissolver (Model 2) is being built to test a new cathode shape, increased anode area, increased circulation at the electrodes to remove gases more efficiently, and to test niobium as a material of construction for the cathode and the fuel-containing basket.

The reliability of a charging chute design [2] in which the fuel elements are originally charged vertically, but are delivered to the dissolver horizontally, was tested in 100 drops each of simulated APPR (2.838- x 2.963- x 27-inch box), PM-3A (0.506-inch O.D. x 33-1/2-inch long tubes), NSP Pathfinder superheater (0.794-inch O.D. x 77-inch long tubes), and Spert III (2.95- x 2.95- x 47-1/8-inch) elements. The data and slow motion pictures from the drops are being evaluated. No visual difficulties were apparent in the tests of this charging chute.

1.2 Voltage Probe Measurements of Polarization

Measurement of the potential at various points within the solution-contact dissolver were made with 1/16-inch diameter stainless steel electrode rods encased in thin-walled plastic tubing. A small area of the rod at the lower end was exposed. Two probes were located at the surface of the platinum anode and the cathode where they measured, in effect, the polarization of the electrode surfaces. Two additional probes were located in milled grooves in the anodic and cathodic surfaces of a stainless steel charge which was shaped to fit the dissolver basket. These probes measured the sum of voltage drops due to the anodic and cathodic polarizations and to the fuel charge itself. The potential drops through the solution gaps were determined from the opposing probes at the respective electrode and charge surfaces. Preliminary measurements indicated that the dissolver required several minutes to reach a steady state temperature.

Two solution compositions were used, one of relatively high acid and low stainless steel concentration, and the second of converse concentrations. Solution inlet temperatures of 19, 29, and 56°C were tested. Overall potentials were varied from 7.7 to 19.4 volts. The results of five series of measurements are shown in Figures 8 through 12. Arrows indicate the variation of current with time (drift) as the dissolver reached steady state. Figure 8 gives the potential measurements at 29°C for the high acid solution. The currents were observed immediately upon reaching the stated total potential. Figure 9 gives similar data at 56°C for a solution of high conductivity. Here it was observed that over a 27 minute period, the dissolver current declined almost 100 amps from

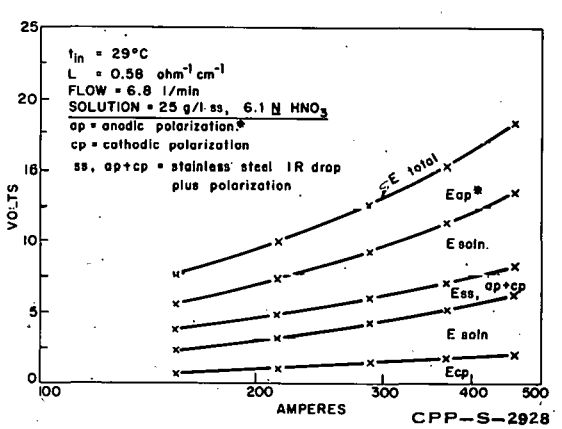

Fig. 8 Potential-current diagram (Series I).

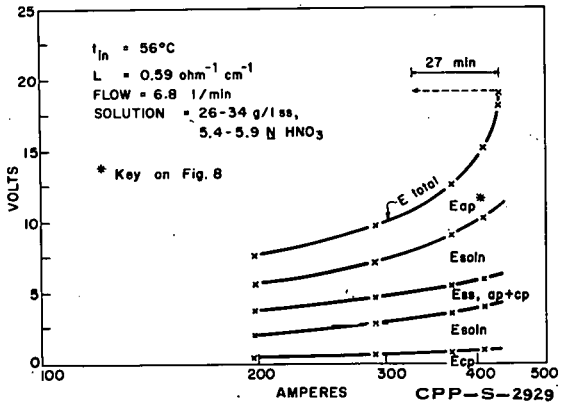

Fig. 9 Potential-current diagram (Series II).

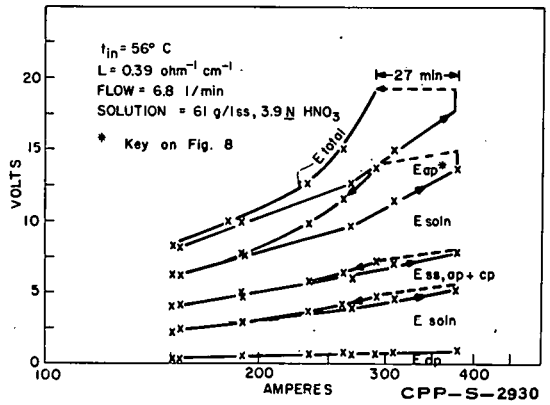

Fig. 10 Potential-current diagram (Series III).

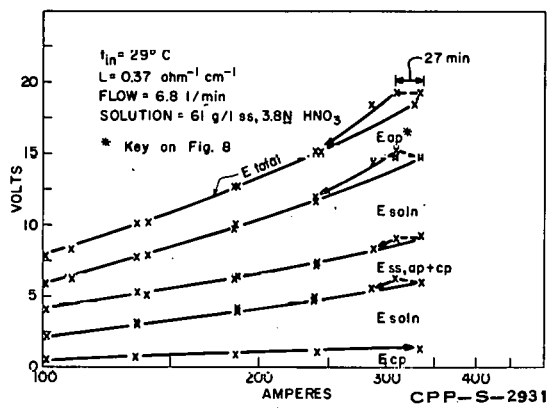

Fig. 11 Potential-current diagram (Series IV).

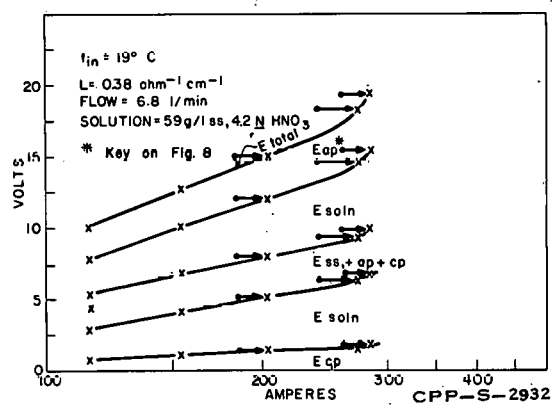

Fig. 12 Potential-current diagram (Series V).

the initial maximum as conditions approached steady state in the dissolver. Figure 10 indicates the behavior of each component of the overall potential drop as a solution of lower conductivity approached steady state. In Figures 10 and 11 current-potential values are plotted for both increasing and decreasing applied voltage; the curve for decreasing voltage reflects the shift in current. Figure 11 shows the relatively small effect of the approach to steady state at 29°C with solution of lower conductance. The data of Figure 12 were taken at a lower temperature, 19°C. Here an upward drift of current was noted at potentials of 15 volts or higher, in contrast to experiments at higher temperature. At 19°C the current increased with time, while at higher temperatures the current decreased with time.

The following observations can be made from these experimental results. When the dissolver is operated below the limiting current density, the majority of the resistance is that from the solution (electrolyte). This may be seen by examining Figures 8 through 11, and was confirmed by replacing a stainless steel product solution with 8N nitric acid; the increase in current at a given voltage corresponded approximately to the gain in conductance of the solution. The cathodic polarization on platinum is small compared to that at the anode.

The variation of the sum of the stainless steel polarizations with current also is rather small.

It is apparent that a major portion of the system resistance is at the anode surface and in the solution adjacent to the anode. This is particularly notable at the highest currents. Here, also, a hysteresis occurs in the current-voltage relationship. The rise to a limiting current density is believed to be associated with gas evolution at the anode surface. The effect is a marked function of temperature above 29°C, lower limiting currents being observed at higher temperatures. Since both the solution resistance and the other polarization resistances decrease with increasing temperature, it would appear desirable to circulate the dissolver solution at higher temperature and, at the same time, cool the anode from an external source. The limiting current density at the anode can then hopefully be raised without lowering the solution conductance.

For solutions of approximately the desired product composition and with an idealized shaped fuel charge, the maximum current density apparently achievable in the present unit is about 1.5 amps/cm^2 of anode at 19.4 volts.

1.3 Stainless Steel Limiting Current Densities

From the foregoing, it appeared that the dissolver unit, when fully loaded with fuel, was limited by the current density of the anode. However, it was not known to what extent the basket must be filled to maintain a given current, ie, at what point the fuel surface becomes limiting. It was hoped that as the fuel area was reduced, a limiting current density would be observed.

A stainless steel charge was fabricated which conformed to the shape of the basket and which had replaceable 1 x 4-1/8-inch horizontal strips attached to both the anode and cathode sides. The metal strips were replaced one by one (from the top down) with Teflon strips. Current and voltage readings were taken as the conducting area facing each electrode was reduced. At the time of the experiment, the circulating solution contained 40 grams of stainless steel per liter and 5.5M nitric acid.

The results of decreasing the fuel area are shown in Figure 13 for both the anodic and cathodic sides. The maximum slope on the anodic (dissolving) side was 6.7 amps/cm^2 of exposed fuel; the maximum slope on the cathodic side was 3.6 amps/cm^2 of exposed fuel. The experiment also was conducted so that the strips on the cathode-side were replaced from bottom to top. In this case a maximum slope of 3.7 amps/cm^2 was found, essentially the same result obtained in the previous experiment. The exposed area of the fuel charge on the anodic side was 146 cm^2, so that this surface could pass a uniformly distributed 980 amperes. On the cathodic side, the available area was 108 cm^2 which, with uniform current distribution,

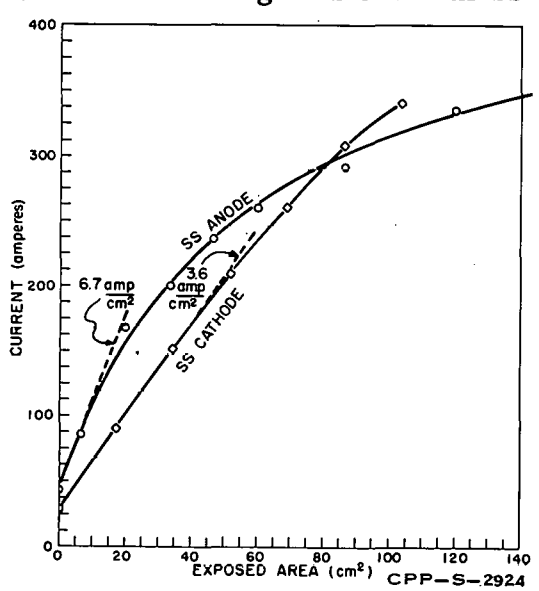

Fig. 13 Variation of current with available stainless steel area for shaped charge at 15 volts.

could pass 389 amperes. The observed current was 340 amperes. These results suggest that the current through the fuel charge facing the anode may become limiting if relatively small improvement can be obtained in current density on the anode itself.

IV. NEW WASTE TREATMENT METHODS

(Section Chiefs: K. L. Rohde, Chemistry; M. E. Weech, Plant Processes)

1. DISPOSAL OF LOW-LEVEL RADIOACTIVE WASTES

(D. W. Rhodes, Problem Leader; M. W. Wilding)

Laboratory studies were continued on the reactions of specific radioisotopes with natural earth materials [a]. The adsorption by earth materials of radioactive cerium and chromium in synthetic MTR pond waste containing EDTA as a possible complexing agent was studied. In addition, the adsorption of cerium from actual MTR pond waste was investigated. Three types of earth materials were used for the experiments; a lignite, a clay material, and the mineral clinoptilolite.

Both cerium and chromium in the chloride form were found to have distribution coefficients of approximately 1000 or greater when EDTA was absent and the pH was in the range 7.0 to 9.0. The presence of EDTA depressed the adsorption of cerium and chromium only slightly.

The adsorption of chromium was considerably less when it was in the form of dichromate ion than when in the form of a cation. The distribution coefficient for dichromate was less than 100 for the clay material and the mineral clinoptilolite, but reached a value of 1000 with lignite in the pH range 7.0 to 9.0. This result is reasonable since both clay and clinoptilolite are almost exclusively cation exchangers while lignite, being an organic material, has anion exchange properties as well.

The distribution coefficients obtained for cerium with actual MTR waste and the three earth materials were actually slightly higher than those obtained using a synthetic MTR waste. The chemical analysis of the actual MTR waste indicated that the concentration of total salts was lower than in the synthetic waste, a factor which may account for the difference in distribution coefficients.

2. DECONTAMINATION OF ALUMINUM NITRATE BY THE FREEZE-MELT TECHNIQUE

(M. E. Weech, Problem Leader; S. J. Horn, P. Burn)

A new tray design was evolved for the freeze-melt apparatus, incorporating changes based upon qualitative observations of the operation of earlier trays [2]. The new trays have forty 3/16-inch diameter transfer holes in the bottom instead of the nine 1/16-inch diameter holes used in the initial design. Also, the heat transfer properties of the tray were altered by changing the coil from a pancake design to an extended helix which distributes the coil area more uniformly through the space between trays. This coil placement cools the acid between trays more efficiently, and more nearly achieves the desired result of crystallization in the solution rather than on the coil surfaces. A further modification

---

[a] Work performed under special arrangement with the ID Health and Safety Division.

included provision of cooling water passages in the bottom portion of the tray which contains the transfer holes. This design will permit freezing of aluminum nitrate on the bottom of the tray and in the transfer holes, thus minimizing bypassing of the trays by crystals that form in the cool solution above and fall directly through the holes. A schematic drawing of the new tray design is shown in Figure 14. The problem of bypassing the trays has not been completely solved; small crystals still fall through the tray holes. This is believed to be due to lags in cooling the somewhat massive tray bottom, suggesting that cooling of the trays should be started sooner than the cooling of the coils above the tray.

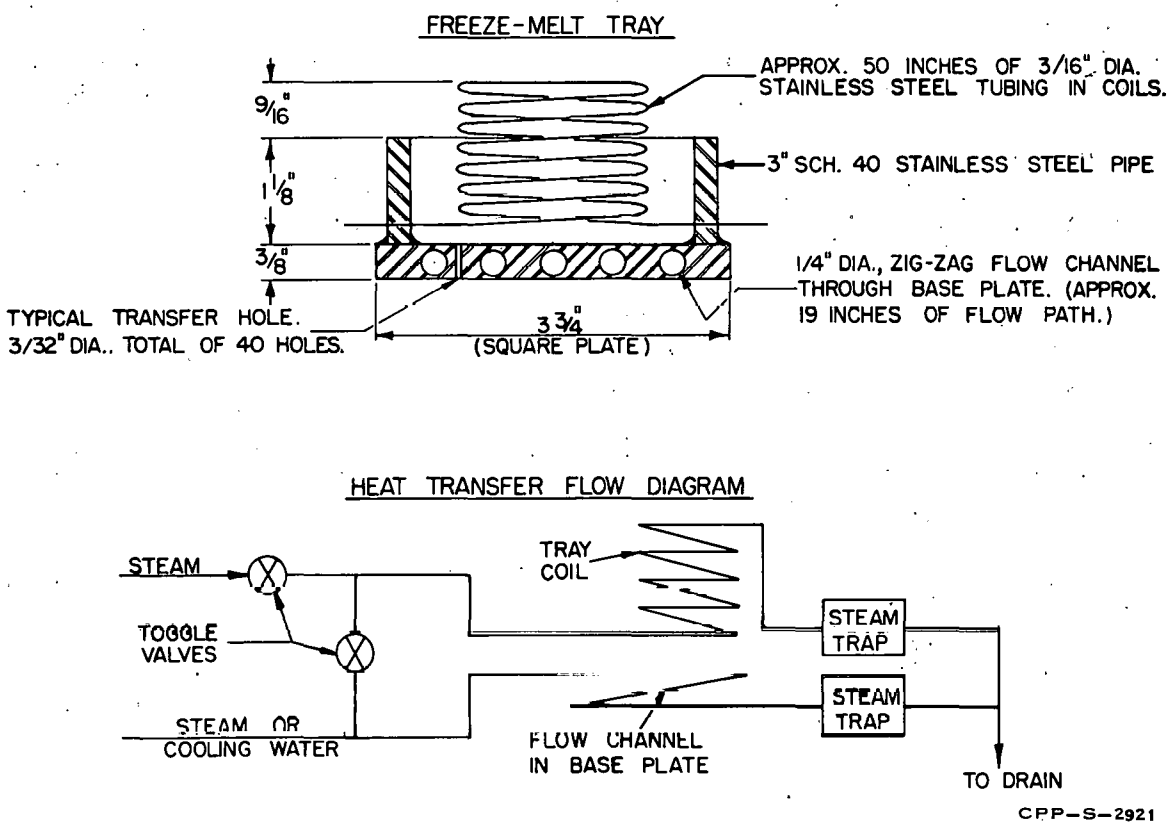

Fig. 14 Schematic diagram of freeze-melt tray and heat transfer system.

The new design trays have a significantly higher throughput than the original trays. However, heat removal on the cooling cycle is still hindered by the tendency of the coils to coat with crystalline aluminum nitrate even though most of the crystals form in the chilled nitric acid surrounding the coils. The coating or fouling of the coil surfaces is produced by the direct freezing of molten salt on the coil surface and also by the slower growth of crystals which settle on the horizontal portion of the coil surface or which become wedged between the coil loops. It is possible to break the crystal coating loose by a brief application of steam to the coil with negligible redissolving or melting of the accumulated crystalline aluminum nitrate; this represents a desirable innovation to the control program. Presently, the tray cooling coil and the tray bottom cooling passages are in parallel; but with the coils and the tray bottom connected independently, it would be possible to thermally cycle the coil without disturbing

the plugs in the transfer holes. Further, by cooling the plate prior to the coil, it should be possible to allow a solid layer of crystalline aluminum nitrate to build up on the tray bottom, thus blocking crystals from bypassing the trays. Modifications are being made in the existing apparatus to include these improvements.

V. WASTE CALCINATION

(Section Chiefs: J. A. Buckham, Development Engineering; K. L. Rohde, Chemistry)

The fluidized bed calcination process for conversion of waste solutions to granular solids [2] has been developed to a point permitting plant-scale operation with actual wastes. The 60-gallon-per-hour Waste Calcining Facility (WCF) has been completely tested with nonradioactive and tracer materials and is being readied for production operation with high-level radioactive aluminum nitrate wastes now stored in tanks at ICPP. No known process or equipment problems remain to be solved, although certain modifications are being made to the WCF to correct potential problems uncovered during cold testing. A detailed analysis of the safety aspects of operation of the WCF is underway. Several studies on mechanistic details of the process were completed this period, and a study of improvement of storage of calciner product by incasement in a fused salt or oxide matrix was initiated.

1. MODIFICATION OF THE WASTE CALCINING FACILITY (WCF)

(L. T. Lakey, Problem Leader; G. E. Lohse, W. P. Palica, R. D. Modrow, D. E. Black, E. D. Cooper, N. Kormanik)

Detailed design of the modifications [2] to the WCF has been completed, and construction work in the facility is underway. Processing of actual ICPP radioactive wastes is anticipated to begin in November 1963. Technical effort is presently concentrated heavily on a detailed analysis of the safety aspects of operating the facility. This analysis has uncovered the need for several minor equipment changes to remove possible hazards; however, no major oversights have been found. A safety analysis report will be published before radioactive processing begins.

2. PILOT PLANT DEVELOPMENT STUDIES

(B. M. Legler, Problem Leader; B. P. Brown, W. B. Kerr, J. C. Petrie)

2.1 Pilot Plant Calciner Operation

One five-day run was made in the two-foot-square pilot plant calciner this period to obtain information on a new feed nozzle designed to produce a coarse spray. Data obtained during this run indicated that the new nozzle was no better than the standard nozzle used in previous runs. The amount of fines generated and elutriated from the bed, while operating at a bed temperature of 300°C and nozzle air-to-liquid volume ratios of 250 and 500, was unchanged from that obtained with the regular feed nozzle.

2.2 Vessel Sparge Test

Test equipment simulating the essential features of the WCF scrubbing solution surge tank (WC-108) was used to study the flow patterns within the tank when sparging a slurry with air. Initial tests with an alumina slurry were made at various air rates and at two different locations of the sparger. Mixing

was incomplete at all air rates when the sparger was located in the same offset position as the sparger in WC-108. Mixing was better, although still incomplete, when the sparger was located at the bottom of the tank. Additional tests will be made to develop a more effective and efficient sparger for use in tanks in slurry service.

3. BEHAVIOR OF MERCURY IN FLUIDIZED BED CALCINATION
(B. R. Wheeler)

Based on recent analyses of samples taken on earlier pilot plant runs, calciner product generated in the WCF at the intended operating temperature, 400°C, is expected to retain about 65 percent of the mercury contained in the feed solution. The balance will probably leave as a vapor with the off-gas. As shown by Figure 15, the quantity of feed mercury retained by the calciner product is a function of the bed temperature at which product is generated. The data were obtained from representative products generated in the two-foot-square calciner from aluminum nitrate simulated waste having two levels of mercury concentration, 0.006M and 0.015M. The percentage retention of mercury in the product appears to be essentially independent of feed mercury concentration at the levels used in the pilot plant unit.

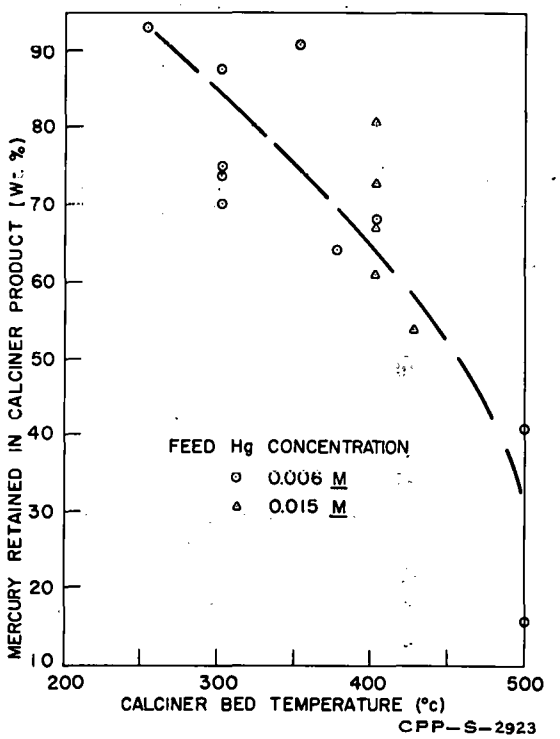

Fig. 15 Effect of calcination temperature on the retention of mercury in calciner product.

Between 20 and 50 percent of the mercury volatilized from the calcination vessel (in addition to that mercury trapped in elutriated particulate matter) is expected to be separated from calciner off-gas by the venturi scrubber for recycle. The scrubber performance, with respect to mercury, appears to depend on the acidity of the scrubber solution or perhaps on the mercury concentration of the off-gas as shown by the data from the two-foot-square calciner listed in Table V.

4. STUDIES OF CALCINATION MECHANISMS
(E. S. Grimmett)

4.1 Particle Growth Rate Studies

Factors affecting the rate of growth of particles in the fluidized bed calcination process have been determined, and a quantitative correlation of particle growth rates has been evolved. Contrary to the usual simplifying

TABLE V

BEHAVIOR OF MERCURY IN TWO-FOOT-SQUARE CALCINER AND VENTURI SCRUBBER

Feed Mercury Concentration (M)	Calciner Bed Temperature (°C)	Superficial Fluidizing Velocity (ft/sec)	Feed Mercury Retained In Calciner Product (wt %)	Percentage of Volatilized Mercury Which Is Separated In Scrubber (wt %)	Acidity of Effluent Scrubber Solution [a] (M)
0.006	500	0.78	41	21	0.02
0.015	400	1.0	61	47	3.24
0.015	400	1.0	73	37	1.98
0.006	425	1.0	54	28	0.95

[a] The off-gas was contacted with fresh water in the venturi scrubber at rates varying between five and ten gallons per thousand actual cubic feet of off-gas. Acidity of effluent scrubber solution is affected by several calcination variables, the relationship of which has not been established.

assumptions made in this connection, the rate of growth of larger particles was found to be greater than that for the smaller particles under all conditions studied.

Particle growth rate was determined to be related to the surface area of the particles in the bed, to the equivalent solid feed rate, to the density of the solid feed material, and to be a function of the particle diameter. This derived relationship is shown in Equation 1,

$$g = \frac{2\,(P/\rho)\,(A + BL)}{\sum_{i=1}^{i=\infty} A_i N_i} \qquad (1)$$

where g is the instantaneous diametral growth rate of a particle of any size L, P is equal to the total mass rate of buildup of calcined feed material on the bed, ρ is the true or particle density of the calcined feed material, A_i is the surface area of a particle in the ith size interval, and N_i is the number of particles in the ith size interval. If the motion of the particles through the feed spray zone in the bed is completely random, then the constant A becomes unity and the constant B becomes zero, and the particle growth rate is independent of particle size. However, if certain forces--such as those associated with high velocity introduction of feed--disturb the usual random mixing associated with a fluidized bed of particles, constants A and B take on other values.

To determine the values of A and B, particle growth rates were determined experimentally by forming identifiable colored shells in the bed particles at various times throughout a calcination run by adding nitrate salts of iron,

nickel, chromium, or copper, to the feed stream for 15 minute periods. At the end of a run, particles from the bed were mounted in plastic and sectioned at or near the particle diameters. This exposed the shells as rings in each particle, and by measuring the effective diameter of each ring the particle growth rate was determined for various times during the run. Figure 16 shows the rings in a typical photomicrograph of a sectioned particle.

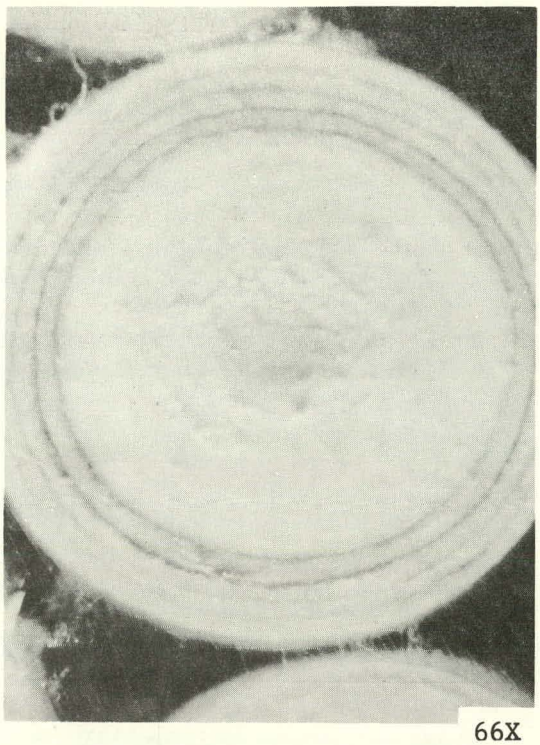

66X

Fig. 16 Photomicrograph of sectioned calciner product particles showing growth rings.

Particle growth rates were determined from data taken on four different calciner runs. Three of these runs were made in a two-foot-square calciner at feed rates ranging from 40 to 90 liters per hour and at bed temperatures ranging from 400 to 500°C. The fourth run was made in a 12-inch diameter calciner at a feed rate of 10 liters per hour and at a bed temperature of 400°C.

Analysis of the data from these four runs shows that particle growth rate is a function of the particle size as well as of the other factors mentioned. It was found that the best values for A and B are 0.542 and 9.12 cm^{-1}, respectively, over the wide range of operating conditions studied.

4.2 Mechanism of Fines Generation

Based on past calcination studies [11, 12], it has been generally concluded that the operating conditions imposed on the feed atomizing nozzle have a considerable influence on the amount of fines generated in a fluidized bed calciner. Although other factors such as bed operating temperature, the physical properties of the bed material, and the fluidizing velocity contribute in varying degrees to the overall production of fines in the calcination process; the nozzle conditions have always had the greatest influence. Fines are generated in the fluidized bed calcination process in several ways as a result of feed introduction: by breakup of bed particles as the energy of the nozzle atomizing air is dissipated, by thermal fracture resulting from contact of the hot particles by the cold spray, and by drying of droplets before they adhere to target bed particles. A mathematical model has been proposed and tested by a chemical tracer technique, which, for the first time, has given a good estimate of the amount of fines generated by spray drying processes as opposed to those generated by attrition processes.

At steady state it is assumed that a constant inventory of elutriatable fines has been built up in the bed, that the rate of elutriation of these fines is constant at the value E, and that the fines inventory is constantly replenished by attrition processes at the rate, A, and by spray drying processes at the rate, S. Thus:

$$A + S = E \tag{1}$$

Upon instantaneous introduction of a soluble chemical tracer into the feed, a layer of chemically-traced product starts forming around the bed particles, and the remainder of the traced feed is spray dried and enters the fines inventory. At any time, t, after introduction of the traced feed, the concentration of the tracer in the attrition-produced fines, X_a, will be a function of the original tracer concentration in the feed, of the thickness of the traced product layer on the particles, and of the depth and extent to which fragments are broken from the bed particles. The concentration of the tracer in the spray dried fines, X_s, however, will depend only on the tracer concentration in the feed. The inventory of elutriatable fines, F, will have a tracer concentration, X_e, which is a function of the magnitude of F, of the relative rates of generation of fines by attrition and by spray drying processes, and of the tracer concentration of each of these types of fines; the concentration of the tracer in the elutriated fines will also be X_e.

A tracer rate balance for the system can be mathematically expressed as

$$\frac{F dX_e}{dt} = AX_a + SX_s - EX_e$$

or

$$\frac{dX_c}{dt} = \frac{AX_a}{F} + \frac{SX_s}{F} - \frac{EX_e}{F} \qquad (2)$$

X_a is some unknown function of time and depends upon many factors. For simplicity, it is assumed that X_a varies exponentially with respect to time, or

$$\frac{dX_a}{dt} = 1/\tau\ (X_s - X_a) \qquad (3)$$

where $1/\tau$ is an unknown time constant.

There are too many knowns in Equations 2 and 3 to permit the rigorous analytical solution of these equations. However, an analog computer technique has been developed from which estimates of the best values of $1/\tau$, S, A, and F can be made. This technique involves trial and error manipulation of computer settings until the best fit is obtained between the experimental values of tracer concentration in the elutriated fines at various times and the computer-drawn curve of X_e versus time.

Based on encouraging trial tests during earlier runs, a series of four tests was devised to test this model in the two-foot-square pilot plant calciner [12]. Calciner operating conditions common to all four tests are given in Table VI, and the various feed nozzle conditions used for each test are given in Table VII. These tests were designed to create conditions of nearly constant rate of production of fines per nozzle by spray drying processes, based on the assumption that the operation of each of the two nozzles in the system does not influence the performance of the other. At the same time, the rate of production of fines by attrition processes was intentionally varied over a wide range by varying the rate of introduction of water into the bed.

TABLE VI

COMMON CALCINER OPERATING CONDITIONS FOR TESTS OF MODEL OF MECHANISM OF FINES GENERATION

Bed temperature, °C	400
Superficial fluidizing velocity, ft/sec [a]	1.0
Feed nozzle caps	Type 347 SS flat faced
Regular feed composition:	
Aluminum nitrate, M	1.29
Nitric acid, M	2.34
Sodium nitrate, M	0.078
Boric acid, M	0.01
Start-up period before tracer introduction	24 hours
Duration of tracer introduction	6 hours
Duration of sampling period following removal of tracer	6 hours

[a] Calculated on the basis of the bed temperature and pressure, but does not include water vapor, nozzle atomizing air, or decomposition products from the feed.

TABLE VII

SUMMARY OF UNIQUE EXPERIMENTAL OPERATING CONDITIONS AND RESULTS FOR TESTS OF THE MODEL OF MECHANISM OF FINES GENERATION

Tracer		Fe	Ni	Cr	Cu
Nozzle A	Fluid	Feed	Feed	Feed	Feed
	Rate (l/hr)	50	50	50	50
	NAR	400	400	400	400
Nozzle B	Fluid	Feed	None	Water	Water
	Rate (l/hr)	50	0	100	50
	NAR	400	0	400	450
S, spray dried fines rate (g/min)		10.0 (5.0 per nozzle)	4.1	6.0	5.1
A, attrition fines rate (g/min)		6.5	4.2	26.2	6.8
F, fines inventory in bed (grams)		600	400	1,000	500
$1/\tau$ ($min^{-1} \times 10^4$)		3.3	10.0	3.3	2.6

The results obtained during these tests are summarized in Table VII. Figure 17 shows typical computer-synthesized curve and the experimental data points obtained during the copper-traced feed experiment. Ignoring a few apparently erroneous experimental points, the match between the computer curve and the data points is excellent.

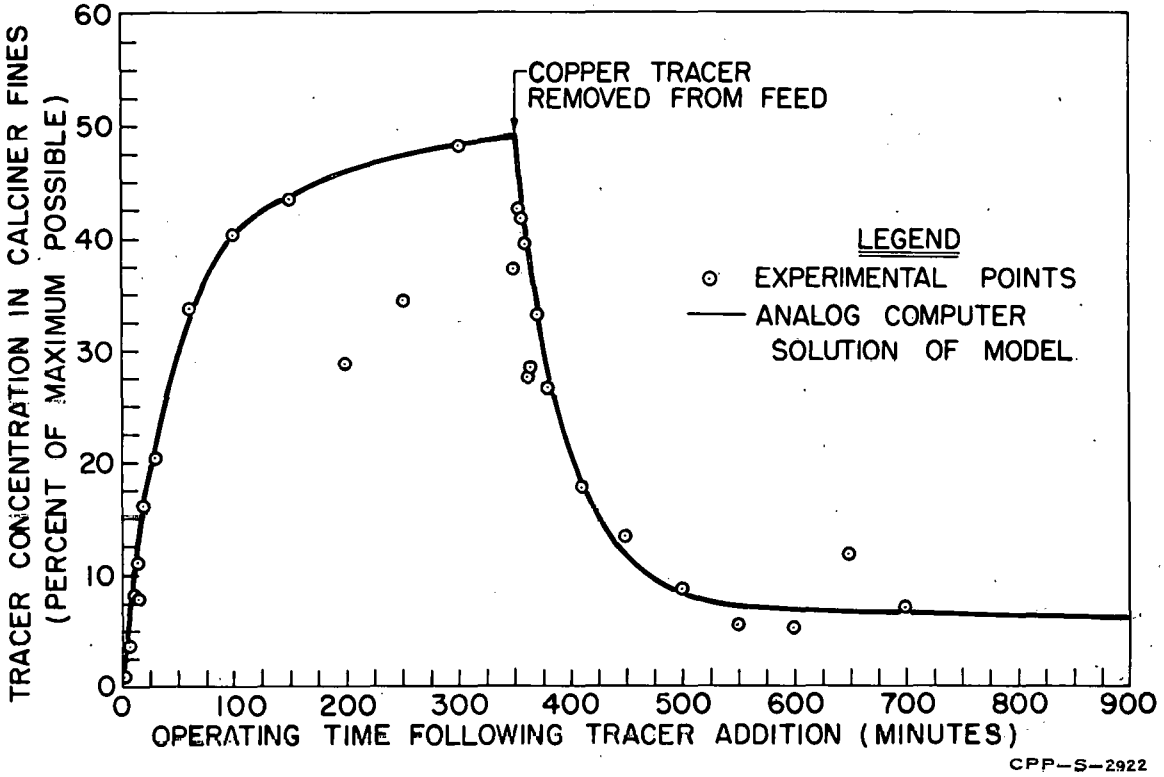

Fig. 17 Comparison of experimental fines generation data with computer solution of mathematically derived fines generation model.

Results of all four of the tests were sufficiently consistent to be encouraging. The rate of production of fines by spray drying processes was reasonably constant at about five grams per minute per nozzle. The rate of production of fines by attrition processes, which had been deliberately varied during the test by use of varying amounts of water injection, ranged from 4 to 26 grams per minute, the larger rates being associated as expected with the larger rates of water injection.

It is of special interest to compare the results of the iron-traced and copper-traced tests. During both of these tests, two nozzles were used and they were operated at nearly identical feed rate and NAR values. However, during the copper-traced experiment, water only was fed through one of the nozzles. As expected, spray dried fines were produced at twice the rate when both nozzles introduced feed during the iron-traced experiment. The product rate of attrition-generated fines was about the same for both runs, also an expected result.

These tests also gave the first quantitative estimate of the magnitude of the fines inventory in the bed. For the 350-kilogram bed, the 400- to 1000-gram inventory of fines amounts to only 0.14 to 0.3 percent of the bed, a quantity too small to be measured accurately by routine screening analyses.

Based on the results of these tests, it is believed that this technique can be used to advantage in future studies made to determine the relative importance, under different operating conditions, of the two primary processes involved in the generation of elutriatable fines. The accuracy of such future tests can be enhanced by improved fines sampling techniques and by extending the start-up period to insure that a steady state exists prior to introduction of the tracer.

5. STORAGE OF CALCINED ALUMINA

(D. W. Rhodes, Problem Leader; B. E. Paige)

Various post-calcination treatments of calcined alumina have been considered to improve its long-term safe storage. One such treatment is the impregnation of all voids--both inter-particle and intra-particle--by a matrix material. This would reduce the leaching rate, increase the thermal conductivity, and make the material free of dusting and readily accountable. Scoping studies have been initiated to develop a matrix which will wet, and therefore coat, the calcined particles and also will have a favorable meltingpoint, thermal conductivity, and cost compared to some of the materials which have already been considered [13, 14].

Materials to be studied were selected on the basis of melting point and solubility, with special attention to cost and availability. These materials, together with some previously studied, were tested for wettability by heating in a muffle furnace with calcined alumina waste from the WCF at temperatures slightly above the melting point of the material. Samples were mounted in plastic and examined under a steroscopic microscope for completeness of coating and penetration. Table VIII is a summary of the results.

In general, the oxides and chlorides wet the alumina in an air atmosphere while the metals do not. Salts and oxides have thermal conductivities of 1-5 x 10^{-3} cal/(sec)(cm)(°C) which is considerably better than air (8 x 10^{-5} cal/(sec)(cm)(°C) which normally fills the calcine voids (about 70 percent total voids). Sulfur is only slightly better than air, having a thermal conductivity of 6 x 10^{-4}cal/(sec)(cm)(°C). In addition, it has a fairly low melting point (119°C). Metals have very good thermal conductivity ranging from 0.1 to 0.5 cal/(sec)(cm)(°C), but based on previous experimental work [15], there is considerable advantage in a matrix which will wet, and therefore coat, the individual calcined particles.

Mixtures of salts and oxides, which have been blended to produce lower melting points or less costly matrices, also have coated the alumina calcine particles. Some mixtures which have been tested include mixtures of lead oxide and vanadium oxide at PbO-to-V_2O_5 weight ratios of 55/45 (M.P. 475°C) and 94/6 (M.P. 760°C), mixtures of lead oxide and lead chloride to PbO-to-$PbCl_2$ weight ratios of 70/30 (M.P. 700°C) and 20/80 (M.P. 430°C), and mixtures of lead sulfide and lead chloride with PbS-to-$PbCl_2$ weight ratios of 20/80 (M.P. 430°C), 35/65 (M.P. 560°C), and 60/40 (M.P. 835°C).

This study shows that some of the salts and oxides should be considered as matrices for the impregnation of the inter- and intra-particle voids in calcined waste during storage. The thermal conductivity will be considerably improved, and the coating will greatly reduce the leaching rate of the calcined

TABLE VIII

WETTABILITY OF CALCINED ALUMINA WITH VARIOUS MATERIALS

Materials Which Wet Calcined Alumina	Melting Point (°C)	Materials Which Do Not Wet Calcined Alumina	Melting Point (°C)
Bismuth Trioxide [a]	820	Aluminium	660
Cupric bromide [a]	504	Antimony trioxide	656
Cupric chloride [a]	422	Lead	327
Lead chloride	501	Lithium fluoride [b]	855
Lead fluoride	855	Potassium fluoride [b]	870
Lead oxide (litharge) [a]	888	Sodium fluoride [b]	990
Lithium carbonate	618	Sodium pyrophosphate	880
Molybdenum trioxide[a]	795	Tellurium	450
Potassium chromate [a]	968	Tin	232
Potassium fluoborate	530	Zinc	420
Sodium tetraborate	741	Zinc orthophosphate	900
Sodium carbonate	851		
Sulfur [a]	119		
Vanadium pentoxide [a]	690		

[a] Penetration of the calcined particle is known to have occurred.
[b] Fused but partially disintegrated the calcined particles

waste. By mixing salts and oxides, there are a large number of prospective matrices which will wet the calcined alumina; consequently, matrices can be selected for various process conditions and properties desired. By blending, low cost mineral dressed ores or refined chemicals could be used to produce mixtures for an impregnation process.

VI. PLANT IMPROVEMENTS
(Section Chief: M. E. Weech, Plant Processes)

1. PLANT INSTRUMENTATION
(M. E. Weech, Problem Leader; L. A. Jobe)

The first cycle product evaporator (H-130) concentrates its feed by a factor of 50:1, the evaporator product must meet a gravity and concentration specification. This creates some unique control problems. A new cascade or feed-forward system [8, 16] (feed rate sets the steam rate while evaporator density adjusts the feed-stream rate controller set point) has been in operation during the last two processing campaigns. A reevaluation of start-up procedures and controller settings was made for this compaign. The new procedures and settings have resulted in excellent performance of this unit.

Control of pulse column interface by valve regulation of raffinate flow has shown that high gain settings (5 to 10) allow rapid recovery from both set point and aqueous feed flow changes, but that at low gain settings the reset mode causes instability. A ten percent set point disturbance caused more oscillation than a 50 percent aqueous feed flow change. Frequency response tests showed the pulse column behaves essentially as a plain capacitance tank, with very little resistance and self-regulation.

2. WASTE SOLVENT CLEANUP FACILITY
(M. E. Weech, Problem Leader; P. Burn, J. W. Garner)

Testing was conducted on a new facility, installed in K cell, for the cleanup of waste diluent and waste solvent prior to burning. The organic material is steam distilled overhead in a packed, jacketed stripper operating at approximately 300°F in order to free it from small amounts of plutonium which, on occasion, made burning and release of the combustion products hazardous.

Both cold and hot feeds were used in these tests, varying from straight diluent (Amsco-125-W) to diluent containing up to eight volume percent TBP. The organic feed rate was held at approximately 75 liters per hour and the steam flow was reduced until a bottom fraction started to accumulate, indicating the minimum steam-to-feed ratio for 100 percent boil-up. There was also a slight drop in the operating temperatures of the stripping column at the point of minimum steam flow.

For pure diluent, a minimum of 0.35 pound of steam per pound of feed was required. For three and eight volume percent TBP in diluent, 0.50 and 1.37 pounds of steam, respectively, per pound of feed were required. The steam-to-feed ratios agree well with the design values.

In the initial hot runs on the stripper with 3-1/4 percent TBP in diluent, the alpha count was dropped from approximately 10^4 c/(min)(ml) to background. Initially differential pressure between the vessel off-gas and waste vent systems

prevented successful operation of the unit; this pressure difference was corrected by installing a seal loop in the aqueous line draining to the vent system. After this correction was made, the unit operated very satisfactorily.

3. NUCLEAR POISONED FUEL STORAGE RACKS
(M. E. Weech, Problem Leader; W. G. Morrison)

DMM nuclear calculations on the IBM-650 computer were used to design a poisoned fuel storage rack for the ICPP irradiated fuel storage basin. The rack as designed provides 92 cadmium-poisoned vertical fuel storage slots 51 inches long, spaced 1.75 inch edge-to-edge in a triangular array, for safe storage of MTR-ETR-ATR-type fuel elements containing up to 250 g U-235 per linear foot of fuel element. Cadmium foil, 20 mils thick, is sandwiched between aluminum tubes 6- and 6.25-inch O.D., respectively. The two aluminum tubes are welded together at the ends to isolate the cadmium from the basin water. The rack is designed for nesting together with identical racks; consequently, the calculations were made for an infinite array in three directions. Nuclear constants for use in the two-group diffusion code (DMM) were obtained on the IBM-650 using the MUFT-R [17] and SOFOCATE [18] codes for the fast groups and thermal group, respectively. No credit was taken in these calculations for fission product or burnable poison content of the irradiated fuel elements. The following tabulations present the calculated eigenvalues for the 6.25-inch O.D. tubes on 1.75-inch edge-to-edge spacing containing varying U-235 loading per foot of fuel element.

Fuel Element Loading, g U-235 per foot	Eigenvalue (k_{eff})
150	0.55
200	0.59
250	0.61

Shielding calculations indicate adequate water cover is available if the poisoned racks are stacked two high.

VII. REPORTS AND PUBLICATIONS ISSUED DURING THE QUARTER

IDO-14604 Evaluation of the Metal-to-Metal Contact Basket-Type Electrolytic Dissolver, H. T. Hahn, J. R. Aylward, M. R. Bomar (May 10, 1963).

IDO-14606 Effect of Alloying Constituents on Aluminum Dissolution Rates, R. D. Fletcher, M. E. Jacobson, R H. Beard (April 15, 1963).

VIII. REFERENCES

1. A. L. Ayers and G. J. Raab, Reprocessing Uranium from the First OMRE Core, IDO-14552 (June 1961).

2. J. R. Bower (ed.), Chemical Processing Technology Quarterly Progress Report, January - March 1963, IDO-14616 (September 1963).

3. J. R. Bower (ed.), Chemical Processing Technology Quarterly Progress Report, April - June 1962, IDO-14593 (September 1962).

4. David Dyrssen and Libor Kuca, "The Extraction of Uranium (VI) with DBP in the Presence of TBP. The 'Synergie' Effect: Substitution or Addition?" ACTA CHEM. SCAND. 14 (1960) pp 1945-56.

5. David Dyrssen, "Extraction of Metal Complexes. XXX. The Dissociation Distribution and Dimerization of Dibutyl Phosphate," ACTA CHEM. SCAND. 11 (1957) pp 1771-86.

6. C. J. Hardy and D. Scargill, "Studies on Mono- and DI-n-Butylphosphoric Acids. II. The Solubility and Distribution of Mono- and DI-n-Butylphosphoric Acids in Aqueous-Organic Solvent Systems," J. INORG. NUCL. CHEM. 11 (September 1959) pp 128-43.

7. K. Alcock et al, "The Extraction of Nitrates by Tri-5n-Butylphosphate (TBP). Part I. The System TBP Plus Diluent Plus H_2O Plus HNO_3," TRANS. FARADAY SOC., 52 (1956) p 39.

8. J. R. Bower (ed.), Chemical Processing Technology Quarterly Progress Report, October - December 1961, IDO-14583 (March 1962).

9. J. R. Bower (ed.), Chemical Processing Technology Quarterly Progress Report, October - December 1962, IDO-14611 (June 1963).

10. Processing of Power Reactor Fuels, Seventeenth Quarterly Progress Report, October 1, 1961 and January 1, 1962, DP-726.

11. D. R. Evans, Pilot Plant Studies with a Six-Inch Diameter Fluidized Bed Calciner, IDO-14539 (April 1961).

12. B. P. Brown et al, Development of a Fluidized Bed Calcination Process for Aluminum Nitrate Wastes in a Two-Foot-Square Pilot Plant Calciner. Part I. Equipment Development and Initial Process Studies, IDO-14586 (June 1962).

13. James M. Morgan, Jr., Donald K. Jamison, and John D. Stevenson (comps. and eds.), Report of the Second Working Meeting on Fixation of Radioactivity in Stable, Solid Media, (Held) at Idaho Falls, Idaho, September 27-29, 1960, TID-7613 (February 1961) p 514.

14. J. R. Bower (ed.), Chemical Processing Technology Quarterly Progress Report, July - September 1962, IDO-14599 (December 1962).

15. J. R. Bower (ed.), Chemical Processing Technology Quarterly Progress Report, July - September 1960, IDO-14540 (February 1961).

16. J. R. Bower (ed.), Chemical Processing Technology Quarterly Progress Report, July - September 1961, IDO-14574 (December 1961).

17. R. A. Grimesey et al, MUFT Revision - A Fast Neutron Spectrum Code for the IBM-650, IDO-16735 (March 1962).

18. R. J. Wagner, 650 SOFOCATE - A Code to Determine Thermal Constants on the IBM-650, IDO-16758 (March 1962).

PHILLIPS
PETROLEUM
COMPANY

ATOMIC ENERGY DIVISION